

Computational Analysis of Amiloride Analogue Inhibitors of *Coxsackievirus* B3 RNA Polymerase

Jessica K Holien^{1**}, Elena V Gazina^{2#}, Robert W Elliott³, Bevyn Jarrott², Craig E Cameron⁴, Spencer J Williams³, Michael W Parker^{1,5} and Steven Petrou^{2,6,7}

¹Structural Biology Laboratory and ACRF Rational Drug Discovery Centre, St. Vincent's Institute of Medical Research, 9 Princes St, Fitzroy, Victoria 3065, Australia

²Florey Institute of Neuroscience and Mental Health, The University of Melbourne, Victoria 3010, Australia

³School of Chemistry and Bio21 Molecular Science and Biotechnology Institute, The University of Melbourne, Parkville, Victoria 3010, Australia

⁴Department of Biochemistry and Molecular Biology, The Pennsylvania State University, University Park, PA 16802, USA

⁵Department of Biochemistry and Molecular Biology, Bio21 Molecular Science and Biotechnology Institute, The University of Melbourne, Parkville, Victoria 3010, Australia

⁶Department of Anatomy and Neuroscience, The University of Melbourne, Victoria 3010, Australia

⁷Centre for Neural Engineering, The University of Melbourne, Victoria 3010, Australia

[#]Authors contributed equally

Abstract

Coxsackievirus B3 (CVB3) is a picornavirus that is responsible for a significant proportion of human myocarditis. However, no antiviral treatment is currently available to treat this disease or indeed any picornaviral infections. Previously it was shown that amiloride and its derivative 5-(*N*-ethyl-*N*-isopropyl)amiloride inhibit the *in vitro* enzymatic activity of CVB3 RNA polymerase (3D^{pol}). Here we measure and compare the inhibitory activity of ten amiloride analogues against CVB3 3D^{pol}. We show that replacement of the 3,5-diaminopyrazinyl moiety of amiloride causes loss of the inhibitory activity, whereas modifications at the 5-amino and guanidino groups increase or decrease potency. Importantly, a combination of substitutions at both the 5-amino and guanidino groups produced a compound that was more potent than its singly modified precursors. The compounds were computationally-docked into available crystal structures of CVB3 3D^{pol} in order to obtain a structural explanation for the activities of the analogues. To create a robust model which explained the biological activity, optimization of one of the CVB3 3D^{pol} crystal structures to take into account active site flexibility was necessary, together with the use of consensus docking from two different docking algorithms. This robust predictive 3D atomic model provides insights into the interactions required for inhibitor binding and provides a promising basis for the development of more potent inhibitors against this important therapeutic target.

Keywords: *Coxsackievirus* B3; Molecular docking; Amiloride; Drug design

Introduction

Coxsackievirus B3 (CVB3) belongs to a large family of positive-strand RNA viruses termed *Picornaviridae*. This family contains numerous human pathogens that cause poliomyelitis, myocarditis, meningitis, hepatitis, common cold and other diseases. Type B coxsackieviruses are responsible for 14-32% of human myocarditis cases, with CVB3 being the most common variant [1]. No antiviral treatment is currently available for any picornaviral infections.

Picornaviral genome replication is catalyzed by the viral RNA-dependent RNA polymerase 3D^{pol}. The three-dimensional structure of 3D^{pol} consists of thumb, palm and fingers domains arranged like a cupped right hand, with an active site located in the palm domain (reviewed in [2,3]). The incoming nucleotide binds directly into the active site via stacking and base pairing to a templating nucleotide, which is followed by conformational changes that reconfigure the active site for catalysis. Two Mg²⁺ ions, coordinated by two aspartic acid residues, are involved in the catalysis: one reduces the pK_a value of the 3'-OH of the primer, allowing its deprotonation and the other orients the triphosphate of the incoming nucleotide. Viral polymerases are excellent targets for antiviral drugs, as demonstrated by the clinical success of drug treatments for human immunodeficiency virus, hepatitis B and C viruses, herpes simplex virus, human cytomegalovirus and varicella zoster virus [4].

We have previously shown that amiloride and its derivative 5-(*N*-ethyl-*N*-isopropyl)amiloride (EIPA) act as non-nucleoside inhibitors of CVB3 3D^{pol} [5,6]. Amiloride was shown to compete

with the incoming nucleotide and Mg²⁺ [5,6]. Computational docking predicted a binding site for amiloride and EIPA in 3D atomic structure of 3D^{pol} [5]. This site was located in close proximity to one of the Mg²⁺ ions and overlapped with the nucleotide binding site, thus providing a rationale for the observed competition [5]. The experimental data suggested that conformational changes are likely to occur in the process of amiloride binding to 3D^{pol} [5,6] and thus crystallization of such complexes may prove difficult, if not impossible. Furthermore, a mutagenesis approach to define key residues in 3D^{pol} that bind these inhibitors is complicated by the fact that the same residues are likely to be important in enzymatic function.

In this work we compare CVB3 3D^{pol} inhibitory activity of ten amiloride analogues to probe the roles of three different structural elements of amiloride: the 5-amino, guanidino and 3,5-diaminopyrazinyl groups. We show that modifications at the 5-amino and guanidino groups modulate the inhibitory activity, whereas replacement of the 3,5-diaminopyrazinyl moiety causes a complete loss

***Corresponding author:** Jessica K Holien, Structural Biology Laboratory and ACRF Rational Drug Discovery Centre, St. Vincent's Institute of Medical Research, 9 Princes St, Fitzroy, Victoria 3065, Australia, Tel: (+61-3) 9288 2480; E-mail: jholien@svi.edu.au

Received June 26, 2014; **Accepted** July 28, 2014; **Published** August 02, 2014

Citation: Holien JK, Gazina EV, Elliott RW, Jarrott B, Cameron CE, et al. (2014) Computational Analysis of Amiloride Analogue Inhibitors of *Coxsackievirus* B3 RNA Polymerase. J Proteomics Bioinform S9: 004. doi:10.4172/0974-276X.S9-004

Copyright: © 2014 Holien JK, et al. This is an open-access article distributed under the terms of the Creative Commons Attribution License, which permits unrestricted use, distribution, and reproduction in any medium, provided the original author and source are credited.

of activity. We optimized one of the available 3D^{pol} crystal structures to allow for active site flexibility and used two alternate docking algorithms to obtain a molecular explanation for the structure-activity relationship seen with the ten amiloride analogues. The resultant model can differentiate between active and inactive amiloride analogues.

Materials and Methods

Amiloride analogues

Amiloride, EIPA, 5-(*N,N*-dimethyl)amiloride (DMA), 5-(*N,N*-hexamethylene)amiloride (HMA), benzamil and 3',4'-dichlorobenzamil (DCB) were purchased from Sigma. *N*'-(5-Chloro-2-hydroxybenzoyl) guanidine (CHG), *N*'-(5-chloro-2-hydroxybenzoyl)-*N*-methyl guanidine (CHMG) and *N*-(5-chloro-2-methoxybenzoyl) guanidine (CMG) were purchased from Specs (Netherlands). *N*-Methyl-benzamil (NMB) and methyl 3-amino-5-hexamethyleneimino-6-chloropyrazinoate were synthesized as described in [7]. 5-(*N,N*-Hexamethylene) benzamil (HMB) was synthesized from methyl 3-amino-5-hexamethyleneimino-6-chloropyrazinoate as follows:

Benzyl guanidine hydrochloride (1.57 g, 8.49 mmol) was added to a solution of sodium (0.17 g, 7.3 mmol) in dry isopropanol (5 mL) and the suspension was stirred for 10 min under N₂. Methyl 3-amino-5-hexamethyleneimino-6-chloropyrazinoate (0.484 g, 1.70 mmol) was added to the suspension and the resulting mixture was refluxed for 15 min. The mixture was cooled and water was added (25 mL). The supernatant was decanted, and the brown residue that remained was washed with water (25 mL). The residue was recrystallized from isopropanol to afford HMB as pale brown crystals (0.219 g, 32%), mp: 169-174°C. ¹H NMR (400 MHz, d₆-DMSO): δ 1.50 (4H, s, H3); 1.74 (4H, s, H2); 3.69 (4H, t, H1); 4.39 (2H, s, benzyl CH₂); 7.27 (1H, s, NH); 7.34 (5H, s, benzyl aromatic); 9.46 (1H, bs). ¹³C NMR (500 MHz, d₆-DMSO): δ 26.16 (hexamethylene C3); 28.07 (hexamethylene C2); 43.86 (benzyl CH₂); 50.15 (hexamethylene C1); 117.61, 120.06 (pyrazine ring); 127.11 (benzyl C4); 127.25 (benzyl C3); 128.43 (benzyl C2); 137.94 (benzyl C1); 151.05, 152.81 (pyrazine ring); 161.20 (C=O); 173.39 (guanidine C=N). HRMS (ESI⁺) *m/z* 402.1799 (C₁₉H₂₅ClN₇O [M + H]⁺ requires 402.1809).

Amiloride, HMA, NMB, HMB, CHG, CHMG and CMG were dissolved in DMSO; EIPA and DCB were dissolved in ethanol; benzamil and DMA in water. Final concentrations of solvents in reactions containing the compounds were 0.1% for amiloride; 0.5% for CHG, CHMG and CMG; 1% for NMB; 2% for EIPA; 2.5% for DCB; 10% for HMA and HMB. Equal concentrations of the solvents were present in the no-compound controls and had no inhibitory effects on CVB3 3D^{pol}.

Determination of IC₅₀ values

To determine the 50% inhibitory concentrations (IC₅₀) of the compounds, an assay of enzymatic activity of CVB3 3D^{pol} was conducted as described in [5]. Reactions contained 1.8 μM 3D^{pol}, 20 μM annealed ³²P-labelled RNA primer-template (5'-GCAUGGGCCC), 10 μM ATP, 5 mM MgCl₂, 50 mM HEPES-NaOH pH 7.5, 2% glycerol, 11 mM 2-mercaptoethanol and test compounds at 0-500 μM concentrations. Reaction mixtures, with or without MgCl₂ and without ATP, were assembled on ice and then incubated for 6 minutes at 30°C prior to addition of ATP or ATP and MgCl₂, respectively. After further incubation at 30°C the reactions were quenched by addition of EDTA and the amount of AMP incorporated into the RNA during the pre-steady-state burst was measured as described in [5]. IC₅₀ values were calculated from the resulting dose-response curves using the equation

$$Y=100/\{1+10^{[(\log IC_{50}-\log X) \times \text{Hill slope}]}\}$$

Where X is compound concentration and Y is the percentage of incorporated AMP, relative to that in no-inhibitor control. The values were calculated using Graph Pad Prism. Compounds that had no effect on 3D^{pol} activity at 500 μM concentration when pre-incubated in the presence of MgCl₂ were not further tested in its absence.

Molecular docking

CVB3 3D^{pol} model preparation: CVB3 3D^{pol} crystal structures (PDB codes: 3CDW [8], 3CDU [8], and 3DDK [9]) were downloaded from the RSCB Protein Data Bank (<http://www.pdb.org/>, [10]) and analyzed for docking suitability (i.e. model completeness, resolution, visual analysis for conformational changes) using Pymol (The PyMOL Molecular Graphics System, Schrödinger, LLC). All structures were aligned by their alpha carbons and for each structure, water and non-physiological ligands (i.e. detergents, salts etc.) were removed. The positions of NTP and Mg²⁺ ions were determined based on superposition of the structures with a closely related poliovirus 3D^{pol} structures as described previously [5]. Each model was then minimized sequentially (hydrogens, side-chains, backbone) under the Tripos Force Field [11], using Sybylx2.0 (Certara L.P, St. Louis, MO, USA) default parameters, with added Gasteiger-Hückel charges [12].

Docking of DCB proved particularly problematic due to steric clashes in all the models. This problem was overcome by firstly taking the docking result of the well behaved benzamil (into 3CDU), adding chlorine atoms to the inhibitor to mimic DCB, and minimizing the resultant complex sequentially (addition of hydrogens, side-chain atoms, backbone atoms) under MMFFs for 10,000 iterations. The ligand was then removed and the optimized protein structure used to form a docking promoter for DCB as described above.

The conformations of the conformationally-variable Lys61 and Lys172 residues were selected from the 3CDU [8] and 3DDK [9] crystal structures. These residues were selected as the HOT area (i.e. the area of greatest interest) for a subset minimization in Sybylx2.0 (Certara L.P, St. Louis, MO, USA), using the Tripos force field [11] until consensus solutions were found.

Ligand docking – Surflex: The two tautomers of each ligand, along with their protonated forms, were minimized under the Tripos force field in Sybylx2.0 (Certara L.P, St. Louis, MO, USA). Docking promoters were constructed for each of the alternate models of CVB3 3D^{pol} in Surflex-Dock (Certara L.P, St. Louis, MO, USA). Each promoter was constructed by selecting a 5Å sphere that encompassed active site residues Ala57, Ile58, Ser60, Lys61, Lys172, Ser173, Arg174, Asp238, Ser289 and Asp329. The float for the promoter was increased to 3Å (default 0) and the promoter threshold reduced to 0.27 (default 0.50). All ligands were docked into each promoter with 5 additional starting conformations per molecule, ring flexibility considered, the density of search increased to 9.0 (default 3.0), and hydrogen and heavy atom protein movement of the receptor allowed. All other parameters were kept as default. The top 20 solutions were analyzed visually in Sybylx2.0 (Certara L.P, St. Louis, MO, USA) and Pymol (The PyMOL Molecular Graphics System, Schrödinger, LLC). A preferred docking solution was one which displayed a significant cluster (>50%) of docking poses in the same orientation. Where a preferred docking solution was found, the ligand-protein complex was minimized under the Tripos force-field for 10,000 iterations and analyzed visually in Pymol (The PyMOL Molecular Graphics System, Schrödinger, LLC), with all figures generated in Pymol. Furthermore, all putative polar interactions and hydrophobic interactions were calculated using the

default parameters in LigPlot + v.1.4.5 [13]. Namely, the maximum hydrogen bond distance (donor-acceptor) was 3.35Å, with the angle (donor-hydrogen-acceptor or donor-acceptor-acceptor antecedent) greater than 90°. For putative hydrophobic interactions, the maximum contact distance was 3.90Å.

Ligand docking – FRED: Using the atomic site detection in fred_receptor (OpenEye Scientific Software, Santa Fe, NM.), all potential binding pockets were selected and used to create a docking receptor for the CVB3 3D^{pol} crystal structure, 3CDU [8]. Omega v2.4.3 (Open Eye Scientific Software, Santa Fe, NM) was used to generate a multi-conformer structure database of all tautomers/protonated forms of the amiloride analogues. These analogues were then docked into the receptor using FRED v3.0.1 (Open Eye Scientific Software, Santa Fe, NM) with the top 20 poses requested. Docking was performed at High, Standard and Low resolution. All other parameters were kept at default. Solutions were analyzed in VIDA v4.1.1 (Open Eye Scientific Software, Santa Fe, NM).

Results/Discussion

Biological activity of amiloride analogues against CVB3 3D^{pol}

We examined the inhibitory activity of amiloride analogues bearing substitutions in three places: the 5-amino, guanidino and 3,5-diaminopyrazinyl groups (Figure 1). The inhibitory effects on the enzymatic activity of CVB3 3D^{pol} were assessed using an assay that measures the incorporation of a single nucleotide into an RNA primer-template by 3D^{pol} during the pre-steady-state burst phase of the reaction [5,14].

CVB3 3D^{pol} was pre-incubated with the RNA primer-template and with various concentrations of the analogues up to 500 M, in the presence or absence of Mg²⁺. Reactions were started by the addition of ATP, or ATP and Mg²⁺, respectively. Addition of Mg²⁺ together with or after the analogue was investigated because previous studies showed that the inhibition of 3D^{pol} by amiloride and EIPA was more pronounced when the compounds were allowed to bind to the enzyme in the absence of Mg²⁺ [5].

Substitutions at the 5-amino group had various effects on the inhibitory activity, with a 9-fold range in IC₅₀ values between EIPA, amiloride, DMA and HMA (Table 1 and Figure S1). Substitutions at the guanidino group also led to variation in inhibitor potencies (Table 1 and Figure S1). Namely, compared to amiloride, DCB was more potent, benzamil less potent, and NMB was inactive. HMB, which bears a combination of substitutions at both the 5-amino and guanidino groups, was more potent than its individually modified precursors, HMA and benzamil (Table 1 and Figure S1). The replacement of the 3,5-diaminopyrazinyl moiety with 2-hydroxybenzoyl or 2-methoxybenzoyl produced inactive compounds (CHG, CHMG and CMG, Table 1).

The inhibitory effects of all active compounds were greater when they were allowed to bind to the enzyme prior to the addition of Mg²⁺ (Table 1 and Figure S1), suggesting overlapping binding sites and a similar mechanism of activity. The effect of Mg²⁺ on inhibitory potency varied between the compounds, with the difference in IC₅₀ values for the addition of compound prior to Mg²⁺ versus simultaneously being 7-fold for amiloride and EIPA, 5-fold for DMA and benzamil, and

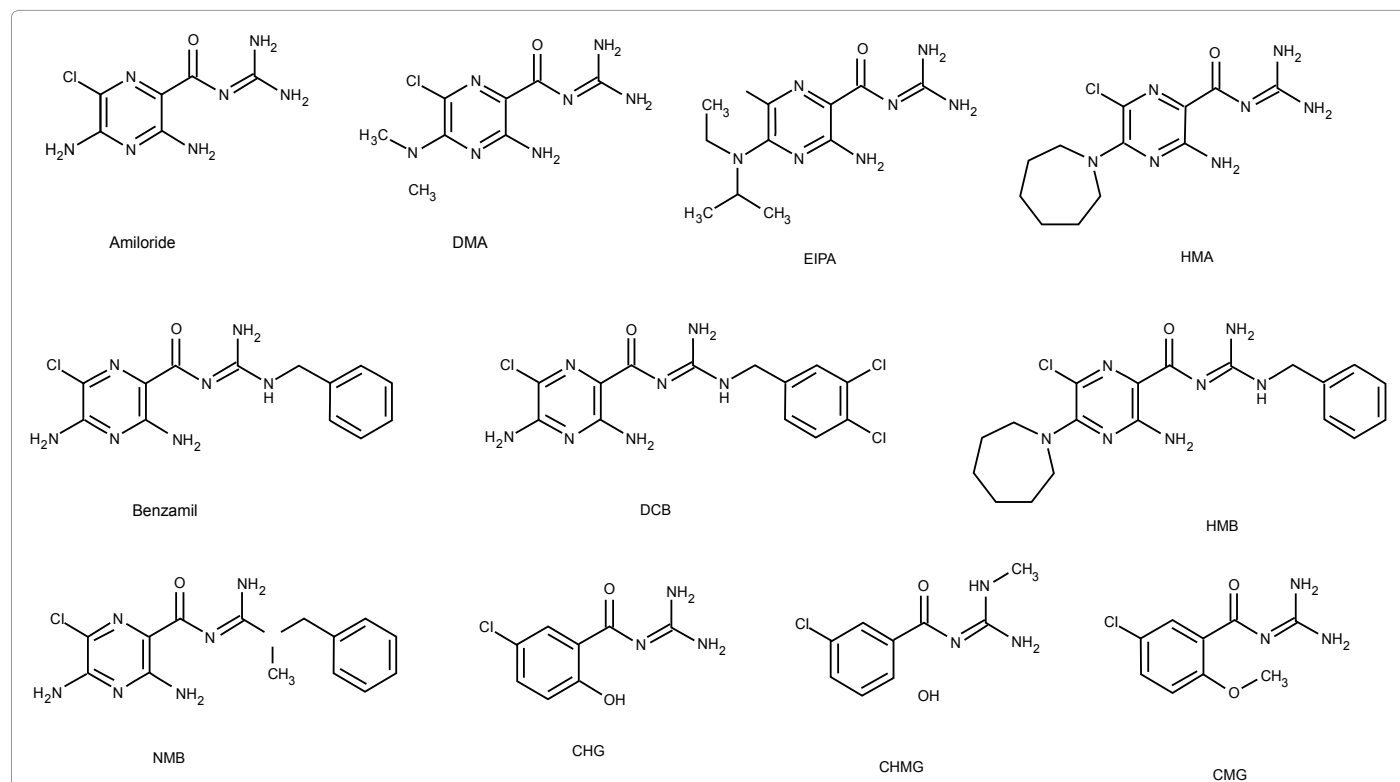


Figure 1: Structures of amiloride analogues.

The structures of the compounds assayed against 3D^{pol} are shown. Although there are numerous tautomeric and protonation states, since the initial docking analysis showed little difference between them, this is the form which will be used throughout the rest of the manuscript. This figure was created using MarvinSketch (<http://chemaxon.com/>).

Compound ID	IC ₅₀ (μM)		Docking Results				
	Mg ²⁺ preincubation	No Mg ²⁺ preincubation	% solutions in preferred cluster	C-Score	Chemgauss 3	Number of Hydrophobic Interactions	Number of Hydrophilic Interactions
Amiloride	139 ± 18	20 ± 1	100	7.13	-57.04	4	7
DMA	424 ± 31	82 ± 29	82	7.12	-53.55	6	7
EIPA	79 ± 10	11 ± 2	50	7.79	-59.66	7	5
HMA	>500 ^a	136 ± 22	70	6.96	-61.22	9	3
Benzamil	255 ± 20	52 ± 11	55	7.8	-62.41	8	5
DCB	45 ± 1	15 ± 3	77	7.53	-58.98	11	7
HMB	>75 ^c	22 ± 4	70	7.59	-58.48	10	6
NMB	inactive ^b	ND	NA	NA	NA	NA	NA
CHG	inactive ^b	ND	NA	NA	NA	NA	NA
CHMG	inactive ^b	ND	NA	NA	NA	NA	NA
CMG	inactive ^b	ND	NA	NA	NA	NA	NA

^aLess than 50% inhibition at 500 μM

^bNo effect up to 500 μM concentration.

^cLess than 50% inhibition at highest possible concentration in solution (75 μM)

ND—not determined

NA—not applicable, i.e. no consistent binding poses were observed

The compounds were pre-incubated with 3D^{pol} and RNA primer/template at different concentrations (0 to 500 μM), either in the presence (left column) or absence (right column) of Mg²⁺, and then reactions were started by addition of ATP or ATP and Mg²⁺, respectively. The IC₅₀ values are mean ± standard error of the mean for 2-4 independent experiments and were determined as described in Materials and Methods. C-score is the consensus scoring function within Surflex (higher scores denote better docking). Chemgauss3 is the atypical scoring function within FRED and is based upon energy (lower values denote better docking).

Table 1: Inhibitory potencies of amiloride analogues in an assay of enzymatic activity of CVB3 3D^{pol} and their scoring functions in Surflex-Dock and FRED algorithms.

3-fold for DCB (Table 1).

Ligand docking

It is generally accepted that no single docking algorithm performs well across all protein targets [15]. Using more than one algorithm builds a consensus that increases the reliability of the results. Two alternate docking algorithms, Surflex-Dock (Certara L.P, St. Louis, MO, USA) and FRED (Open Eye Scientific Software, Santa Fe, NM), were used in this study. The Surflex-Dock algorithm uses an active site protomol as a target for ligand docking. Numerous poses of the ligand are generated and placed into the protomol and scored using the Surflex scoring functions [16]. The FRED algorithm (Open Eye Scientific Software, Santa Fe, NM) performs a systematic and exhaustive search of all possible ligand poses, which need to be generated separately using a program such as Omega (Open Eye Scientific Software, Santa Fe, NM). It then filters and optimizes the poses using the Chemgauss4 scoring function [17]. Both programs rank the compounds based upon the calculated scoring functions.

Picornaviral 3D^{pol} undergoes significant conformation changes during the catalytic cycle: the incoming nucleotide binds to an “open” conformation of the enzyme-RNA template complex, its binding triggers the closure of the active site to form a catalytically competent “closed” conformation, which reopens after the nucleotide addition [9,18]. One method to enrich computational docking and to accommodate targets prone to conformational changes is to use an ensemble of protein structures [19]. Three crystal structures of CVB3 3D^{pol} were used in docking experiments; PDB codes: 3CDW [8], 3CDU [8], and 3DDK [9] (<http://www.pdb.org> [10]). All structures have comparable resolution and completeness and belong to the same space groups. The only notable differences between the three are that 3CDW and 3CDU were crystallized from the Nancy strain of *Coxsackievirus*, whilst 3DDK was crystallized from a different strain. Also, 3CDW was co-crystallized with a VPg primer. The recently published elongated structures [20] were not included in this venture, although visual analysis suggests they would have similar docking limitations for

this project as the 3DDK structure (see below). All of the amiloride analogues were initially docked into the previously-defined amiloride binding pocket [5] of all three CVB3 3D^{pol} structures, in the presence and absence of Mg²⁺, using Surflex-Dock in Sybylx2.0 (Certara L.P, St. Louis, MO, USA). In the presence of Mg²⁺, no consistent cluster of solutions could be obtained for any of the ligands. When Mg²⁺ was absent in the 3CDW and 3CDU crystal structures, none of the inactive compounds showed a consistent cluster of solutions, whereas six out of seven active compounds (except DCB – see below) docked and clustered in an analogous manner in the nucleotide binding site, overlapping the Mg²⁺ binding site (Figure 2). These docking solutions were almost identical to the one previously described for amiloride and EIPA [5]. All tautomers and protonated forms of these ligands docked in an analogous way, with little difference in the scoring function (C-score) value.

For the 3DDK structure, five active compounds (except DCB and DMA) showed a consistent docking solution for over 50% of the top 20 poses, but the docking orientations were almost perpendicular compared to the solutions obtained for the 3CDU/3CDW structures. A possible reason for docking differences is revealed from a comparison of the active sites in all three crystal structures: there are prominent side-chain movements of Lys172 and Lys61 between the 3CDW/3CDU and 3DDK structures. A subset energy minimization was performed on the 3DDK and 3CDU structures where the two lysine residues were allowed to move. The side-chain of Lys172 in both minimized structures moved towards the position found in 3CDU. However, the minimization of Lys61 resulted in a range of orientations, suggesting that a large amount of movement of this side-chain is possible (Figure 3). This finding is supported by high (>40Å²) temperature factors (a crystallographic measure of side-chain flexibility and/or disorder) for Lys61 in both the 3CDU and 3DDK crystal structures. Analysis of the electron density maps derived from the crystallography studies (calculated from the deposited structure factors in the relevant PDB entries) is consistent with at least two alternate conformers of Lys61 in the 3DDK structure, and there is poor electron density for the

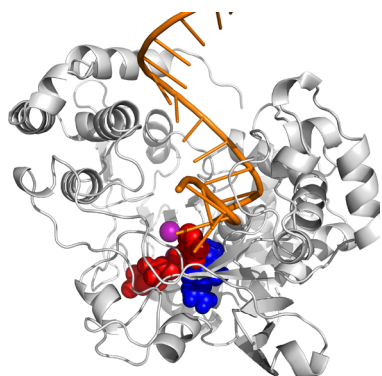


Figure 2: Docking of amiloride analogues.

Our optimized CVB3 3D^{pol} structure (based upon PDB code: 3CDU, [8]) is shown as grey cartoon. The blue spheres denoting amiloride, show a partial overlap in the binding site to the previously reported [5] position of ATP (red spheres), and displays a distinct overlap with the previously determined position of the Mg²⁺ atoms (purple spheres, PDB code: 3OL7, [18]). The position of the RNA template (orange cartoon, PDB code: 3OL7, [18], not used in docking experiments) is also shown.

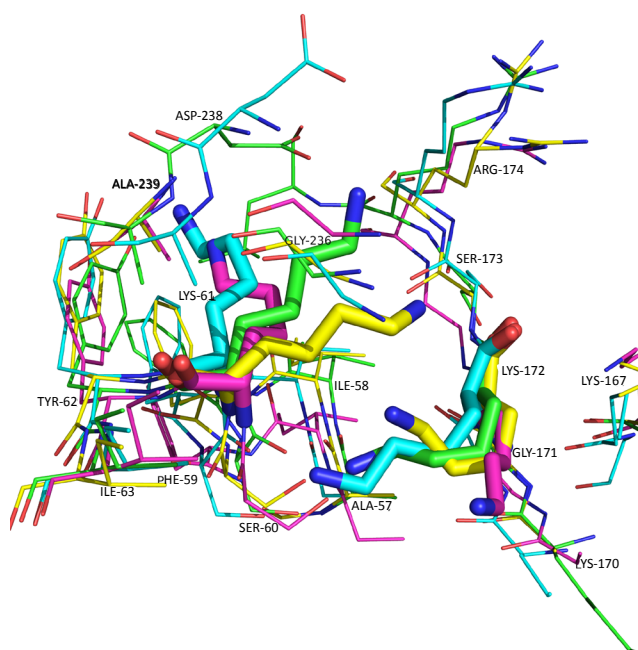


Figure 3: Energy minimization of Lys61 and Lys172.

Displayed is the residues within 4Å of Lys 61 and Lys172 (highlighted with sticks) from 3DDK (magenta carbons) and 3CDU (yellow carbons) plus their minimized versions shown in cyan carbons and green carbons, respectively. There is significant movement between the structures for many of the residues in this region however, only the wide variety of possible side-chain orientations for Lys61 and Lys172 seemed to significantly impact the docking.

side-chain in the 3CDU structure. Most crystal structures of other *Picornaviridae* 3D^{pol} (e.g. poliovirus), including the recent elongated Coxsackievirus complexes [20] have the side-chain of Lys61 forming the NTP tunnel wall, allowing it to engage in a salt bridge with Glu177. However, although the side-chain of Lys61 in the 3DDK structure is in a similar position to that seen with other *Picornaviridae* structures, there is a rotation about the Cα-Cβ bond of Glu177, orientating the side-chain so there is no salt bridge. Based on these data and the fact that a larger number of active compounds docked in an analogous

manner into the 3CDU/3CDW structures when compared to the 3DDK structure, 3CDU was chosen as a preferred docking receptor.

Surprisingly, DCB did not dock in a consistent, clustered manner although it is structurally similar to benzamil. Inspection of the benzamil-3CDU complex revealed that the phenyl group spans the full extent of the binding pocket suggesting the chlorine atoms on the phenyl group of DCB might clash with residues Glu177 and Ser289. Previously published experimental data suggested that amiloride is a slow inhibitor, and hence it's binding to CVB3 3D^{pol} is likely to involve conformational changes [5]. In poliovirus 3D^{pol}, the equivalent residue to Ser289 (Ser288) is important for NTP ribose recognition and active site closure, and as such it is repositioned during the conformational changes that lead to catalysis [18,21]. This residue has been observed in multiple conformations, in various crystal structures of *Picornaviridae*. To allow for the flexibility of Ser289 in the model, the two chlorine atoms were added to the phenyl group of benzamil in the benzamil-3CDU complex, and the resulting model was minimized. The ligand was then removed and the optimized structure was used as a docking receptor for all amiloride analogues. Each ligand bound complex was allowed to minimize for 10,000 iterations, allowing for further movement of the side-chains of the residues.

All active compounds docked to the optimized CDU structure so that they have a hydrogen bond between a nitrogen atom of the guanidino group and the backbone of Ile58, and another bond between the 3-amino group and the backbone of Leu175 (Figure 4 and Figure S2). Additional interactions for each compound are shown in Figure 3 and detailed in Table S1. Although the docking model solutions are similar to those described previously for amiloride and EIPA [5], some of the predicted interactions are now different in the optimized model. For example, the two hydrogen bonds to the backbone of Ile58 were previously reported as two hydrogen bonds to Ala57 and Ser60 [5]. Since the optimized model described here differentiates between the active and inactive amiloride analogues, we believe the new approach supersedes the previous approach and the accompanying conclusions.

Analysis of the top 20 ranked poses for each compound revealed that DCB and benzamil had a small cluster (3 out of 20) of solutions in an alternate binding mode. To analyze the potential of alternate binding modes and/or binding sites not identified by the Surflex-Dock program (Certara L.P, St. Louis, MO, USA), we docked all compounds into the refined 3CDU structure using the OE Docking suite, which includes FREDv3.0.1 (Open Eye Scientific Software, Santa Fe, NM). The results for all three FRED resolutions were identical to those described above, with no consistent cluster of binding poses observed for inactive compounds, and all of the active compounds docking to overlap the nucleotide binding site, consistent with the results obtained using Surflex-Dock. The consensus between the two docking algorithms was consistent with the predicted binding mode.

Numerous studies have examined the ability of different docking programs to predict ligand affinity to an extensive array of protein targets, with the consensus being that docking is suited to identify activity, but does not effectively rank affinities [15]. Additionally, the narrow range of potencies (differences in IC₅₀ values of less than 10-fold) for the active compounds here precluded a meaningful correlation between the docking scores and the potencies of the active compounds (Table 1).

The docking models developed herein provide a rationale for most of the biological data. Strikingly, none of the inactive analogues

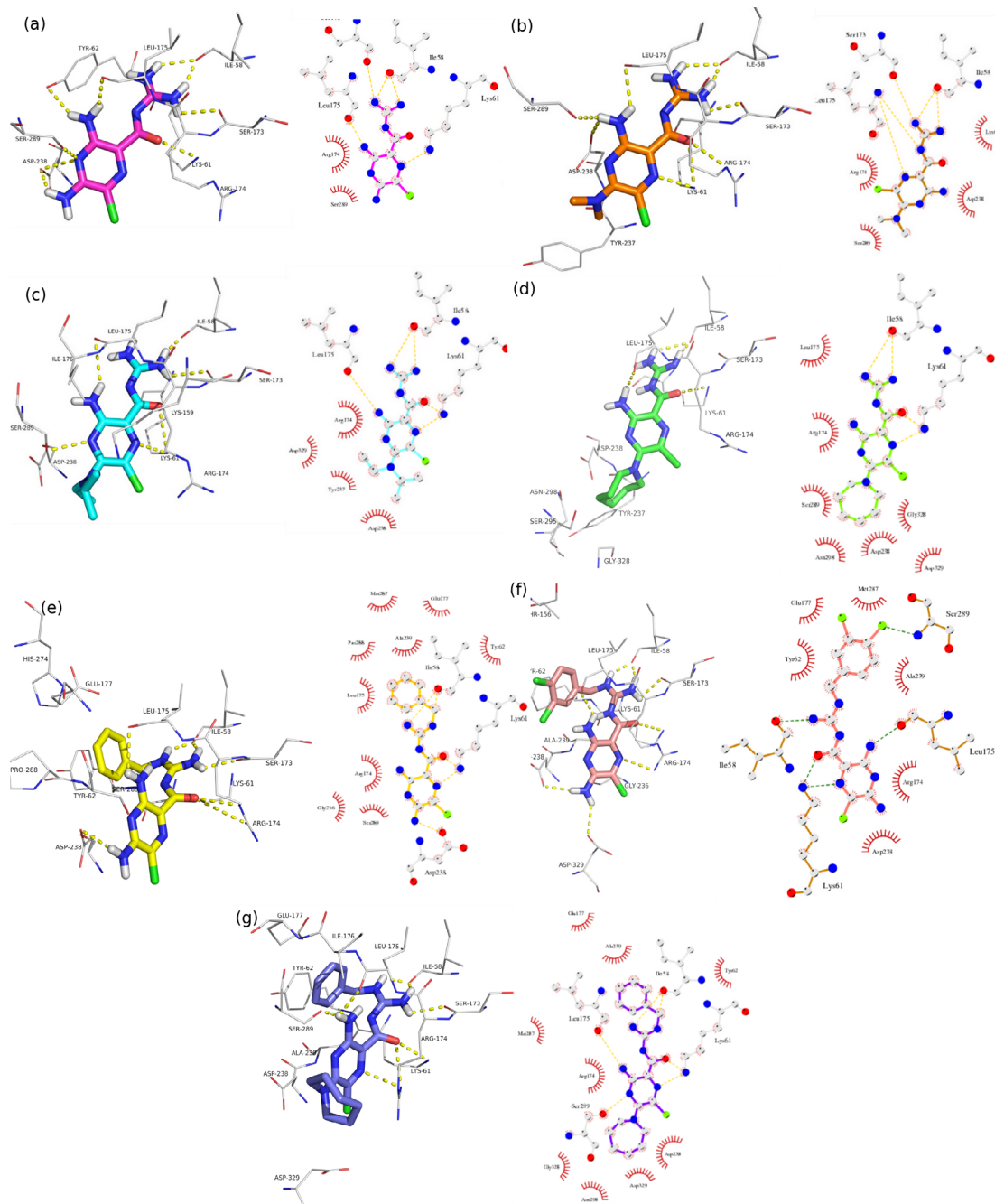


Figure 4: Inhibitor docking to 3D^{pol}.

All active compounds interact in the same general orientation in the nucleotide binding site. The residues involved in significant interactions with inhibitors are shown (grey sticks) with polar interactions indicated as yellow dashed lines. The schematic 2D representations shown in the right column were created by LigPlot[®] v1.4.2 [13] with hydrophobic interactions shown as red semi-circles with lines radiating out in the direction of the interaction. **(a)** Amiloride (magenta carbons); **(b)** DMA (orange carbons); **(c)** EIPA (cyan carbons); **(d)** HMA (green carbons); **(e)** Benzamil (yellow carbons); **(f)** DCB (peach carbons); and **(g)** HMB (purple carbons).

were able to dock in a consistent manner, which can be rationalized by considering the docking orientation. For example, the additional methyl group in NMB would clash with the backbone of Ile58 and remove what appears to be an important hydrogen bond. For CHG, CHMG, and CMG, many hydrogen bonding interactions are lost with the exchange of the nitrogen atoms to carbons in the pyrazine ring and the loss of 3,5-amino groups. These interactions are obviously essential for the CVB3 3D^{pol} inhibitory activity of this compound

class. Furthermore, the boundaries of the binding pocket have been probed with larger active compounds such as DCB and HMB. Also, the 5-ethylamino group of EIPA, when compared to the 5-methylamino group of DMA, allows for extra hydrophobic interactions with Lys159 and Ile176 (Figure 4b and 4c).

In conclusion, we report an initial structure-activity relationship for amiloride analogues that reveals that the 5-amino and guanidino groups of amiloride individually modulate potency of CVB3 3D^{pol}

inhibition and in combination can have an additive effect. We have investigated several approaches to molecular docking and have shown that the choice of the initial protein model plays a significant role in the ability of two alternate docking programs to find consistent solutions. The optimized docking model described here provides insight into the interactions required for inhibitor binding and allows the distinguishing of active versus inactive compounds. Two interactions have been identified that appear to be critical for inhibitory activity: a hydrogen bond between a nitrogen atom of the guanidino group of the active inhibitor and the backbone of Ile58, and a hydrogen bond between the 3-amino group of the inhibitor and the backbone of Leu175. The optimized molecular model can now be used to design more potent amiloride analogues to explore the structure-activity relationships of this compound class and facilitate the development of drugs for the treatment of CVB3 infections.

Acknowledgement

This work was supported by the Australian Research Council grant DP0987855 and National Institute of Allergy and Infectious Diseases (NIAID, NIH) grant AI045818 to C.E.C. Infrastructure support from the National Health and Medical Research Council (NHMRC) Independent Research Institutes Infrastructure Support Scheme and the Victorian State Government Operational Infrastructure Support Program to St Vincent's Institute are gratefully acknowledged. Jessica K. Holien is a joint Cure Cancer/Leukaemia Foundation Postgraduate Fellow, Michael W. Parker is a NHMRC Senior Principal Research Fellow and Steven Petrou is a NHMRC Senior Research Fellow.

References

1. Andréoletti L, Lévêque N, Boulagnon C, Brasselet C, Fornes P (2009) Viral causes of human myocarditis. *Arch Cardiovasc Dis* 102: 559-568.
2. Lescar J, Canard B (2009) RNA-dependent RNA polymerases from flaviviruses and Picornaviridae. *Curr Opin Struct Biol* 19: 759-767.
3. Ferrer-Orta C, Agudo R, Domingo E, Verdaguer N (2009) Structural insights into replication initiation and elongation processes by the FMDV RNA-dependent RNA polymerase. *Curr Opin Struct Biol* 19: 752-758.
4. De Clercq E (2011) A 40-year journey in search of selective antiviral chemotherapy. *Annu Rev Pharmacol Toxicol* 51: 1-24.
5. Gazina EV, Smidansky ED, Holien JK, Harrison DN, Cromer BA, et al. (2011) Amiloride is a competitive inhibitor of coxsackievirus B3 RNA polymerase. *J Virol* 85: 10364-10374.
6. Harrison DN, Gazina EV, Purcell DF, Anderson DA, Petrou S (2008) Amiloride derivatives inhibit coxsackievirus B3 RNA replication. *J Virol* 82: 1465-1473.
7. Cragoe EJ Jr, Woltersdorf OW Jr, Bicking JB, Kwong SF, Jones JH (1967) Pyrazine diuretics. II. N-amidino-3-amino-5-substituted 6-halopyrazinecarboxamides. *J Med Chem* 10: 66-75.
8. Gruez A, Selisko B, Roberts M, Bricogne G, Bussetta C, et al. (2008) The crystal structure of coxsackievirus B3 RNA-dependent RNA polymerase in complex with its protein primer VPg confirms the existence of a second VPg binding site on Picornaviridae polymerases. *J Virol* 82: 9577-9590.
9. Campagnola G, Weygandt M, Scoggin K, Peersen O (2008) Crystal structure of coxsackievirus B3 3Dpol highlights the functional importance of residue 5 in picornavirus polymerases. *J Virol* 82: 9458-9464.
10. Beran HM, Westbrook J, Feng Z, Gilliland G, Bhat TN, et al. (2000) The Protein Data Bank. *Nucleic Acids Res* 28: 235-242.
11. Clark M, Cramer RD, Van Opdenbosch N (1989) Validation of the general purpose tripos 5.2 force field. *Journal of Computational Chemistry* 10: 982-1012.
12. Streitwieser A (1961) *Molecular orbital theory for organic chemists*: Wiley.
13. Wallace AC, Laskowski RA, Thornton JM (1995) LIGPLOT: a program to generate schematic diagrams of protein-ligand interactions. *Protein Eng* 8: 127-134.
14. Arnold JJ, Cameron CE (2000) Poliovirus RNA-dependent RNA polymerase (3D(pol)). Assembly of stable, elongation-competent complexes by using a symmetrical primer-template substrate (sym/sub). *J Biol Chem* 275: 5329-5336.
15. Moitessier N, Englebienne P, Lee D, Lawandi J, Corbeil CR (2008) Towards the development of universal, fast and highly accurate docking/scoring methods: a long way to go. *Br J Pharmacol* 153 Suppl 1: S7-26.
16. Jain AN (2003) Surflex: fully automatic flexible molecular docking using a molecular similarity-based search engine. *J Med Chem* 46: 499-511.
17. McGann MR, Almond HR, Nicholls A, Grant JA, Brown FK (2003) Gaussian docking functions. *Biopolymers* 68: 76-90.
18. Gong P, Peersen OB (2010) Structural basis for active site closure by the poliovirus RNA-dependent RNA polymerase. *Proc Natl Acad Sci U S A* 107: 22505-22510.
19. Huang SY, Zou X (2010) Advances and challenges in protein-ligand docking. *Int J Mol Sci* 11: 3016-3034.
20. Gong P, Kortus MG, Nix JC, Davis RE, Peersen OB (2013) Structures of coxsackievirus, rhinovirus, and poliovirus polymerase elongation complexes solved by engineering RNA mediated crystal contacts. *PLoS One* 8: e60272.
21. Sholders AJ, Peersen OB (2014) Distinct conformations of a putative translocation element in poliovirus polymerase. *J Mol Biol* 426: 1407-1419.

This article was originally published in a special issue, **Computational Intelligence in Bioinformatics** handled by Editor(s). Dr. Jean-Christophe Nebel, Kingston University, London, UK